

Phonons in the Commensurate Monolayer of D₂ on Graphite

V. L. P. Frank,⁽²⁾ H. J. Lauter,⁽¹⁾ and P. Leiderer⁽²⁾

⁽¹⁾*Institute Laue Langevin, F-38042 Grenoble Cedex, France*

⁽²⁾*Institute of Physics, J. Gutenberg University, D-6500 Mainz, Federal Republic of Germany*

(Received 1 December 1987)

The in-plane phonons of the commensurate monolayer of deuterium adsorbed on graphite have been measured. They show evidence for dispersion rather than completely localized mode character. In addition to the phonon gap a transverse and a longitudinal zone-boundary phonon could be measured. The coupling constants between the adsorbed molecules themselves and between molecules and the substrate have been deduced. It is found that the in-plane coupling to the substrate is nearly 10 times stronger than the coupling to neighboring molecules.

PACS numbers: 68.35.Ja, 61.12.Ex, 67.70.+n

Quantum gases adsorbed on graphite are systems of considerable experimental and theoretical interest, in particular for the study of phase transitions of the two-dimensional (2D) quantum systems. These systems are important for the study of the influence of quantum aspects and for comparison with the behavior of the adsorbed heavier noble gases. For a precise understanding of such phenomena it is necessary to know the details of the dynamics of the adsorbate on the graphite substrate.

The phase diagram of monolayers of deuterium (D₂) adsorbed on graphite has been studied extensively by neutron scattering,¹ heat capacity,² nuclear magnetic resonance,³ and low-energy electron diffraction.⁴ D₂ on graphite forms a commensurate ($\sqrt{3} \times \sqrt{3}$)R30° structure (*c* phase) for an adequate density at low temperatures ($T < 18$ K) as do all the quantum gases adsorbed on graphite (see, e.g., Ref. 2b). This occurs even though the mismatch of the nearest-neighbor distance (a_{nn}) of the commensurate 2D structure (4.26 Å) and that of the zero-pressure 3D solid (3.607 Å; a_{nn} in the hcp plane)⁵ is nearly 20%. It is the high compressibility due to the zero-point motion of the D₂ molecules which makes this structure energetically favorable.⁶ However, a first interpretation of the measured phonon spectra of the adsorbed D₂ will be performed in a classical way as was done for 3D D₂.⁵ Useful information is already obtained by the classical model. A comparison to a self-consistent phonon calculation⁷ is included.

The out-of-plane oscillation of the D₂ molecules is dominated by the variation of the D₂-graphite potential in the direction normal to the graphite surface plane. The in-plane oscillations in the commensurate phase are mainly given by the corrugation of the D₂-graphite potential along the surface. In this work only the in-plane oscillations have been measured. In the first inelastic-neutron-scattering (INS) experiments¹ only an "Einstein mode" could be detected in the commensurate phase and no dispersion of the phonons could be seen. Thus the model held that the molecules oscillate in the potential wells caused by the corrugation of the graphite and that

the interaction between the molecules is negligible. Already in our previous measurement⁸ it was seen that the width of the Einstein-mode peak is larger than the resolution of the instrument. It is the aim of this work to show for the first time that higher-resolution studies can detect a dispersion and that a ratio can be deduced between the amount of the in-plane interaction between the adsorbed molecules themselves and that between the molecules and the substrate given by the corrugation. These results are essential not only for the understanding of the commensurate phase itself, but also to interpret the excitations found in the adjacent domain-wall phases⁸ and to model properly the commensurate-to-incommensurate transition. It is difficult to obtain these results by experimental techniques other than INS.

The inelastic neutron spectra were taken with the three-axis spectrometer IN3,⁹ with a fixed final energy ($E_F = 0.99$ THz), a Be filter in front of the analyzer, and a horizontally focusing analyzer.¹⁰ The energy resolution across the elastic line was 0.033 THz FWHM. It worsens with a nonzero energy transfer and increases to about 0.057 THz at 1 THz energy transfer. The sample cell was filled with Papyex¹¹ sheets oriented such that the *c* axis of the graphite was perpendicular to the neutron-scattering plane. This geometry favors the measurement of the in-plane excitation. The densest monolayer consisted of 494 cm³ STP D₂.

The scans in Fig. 1 show inelastic neutron studies which are taken at a coverage of a completely filled commensurate layer and at a temperature of 4 K. The scattering from the sample without adsorbed D₂ was subtracted as the background. The graphite sample is essentially a 2D powder, because the in-plane crystallographic directions are not oriented. Thus the measured signal consists of a directional summation over all phonons for which the scattering triangle closes. The path along which the phonons are collected in the reciprocal space is a circle with a radius given by the total momentum transfer Q (see Fig. 2). Those phonons for which a singularity in the density of states exists along this path

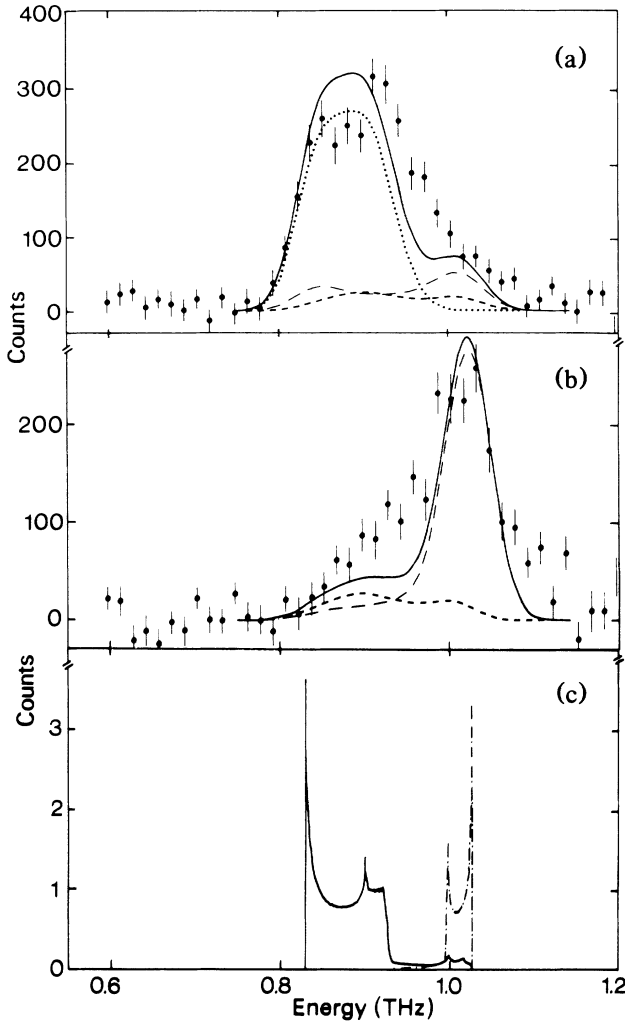


FIG. 1. Neutron inelastic data for (a) $Q = 1.70 \text{ \AA}^{-1}$ and (b) $Q = 0.85 \text{ \AA}^{-1}$ for D_2 on graphite in the commensurate phase (the background is already subtracted). The solid line shows the calculated line shape, the dotted line is the contribution from the transverse mode, the dash-dotted line is the contribution from the longitudinal mode, and the dashed line is the incoherent scattering. (c) Calculated line shapes for the spectra shown in (a) and (b) before convolution with the spectrometer energy resolution function (the Q resolution has already been included in the calculation). The solid line represents the spectra for $Q = 1.70 \text{ \AA}^{-1}$ and the dash-dotted line for $Q = 0.85 \text{ \AA}^{-1}$. The different peaks can be identified by comparison with Fig. 3. For example, the low-energy peak corresponds to the energy gap at the Γ point.

contribute most to the signal. The scan taken at a momentum transfer $Q = 1.70 \text{ \AA}^{-1}$ focuses on the phonons at the zone center and the transverse phonons at the zone boundary (see Fig. 2 and Taub *et al.*¹²). These phonons are found in Fig. 1(a) at about 0.86 and 0.93 THz, respectively. The scan taken at $Q = 0.85 \text{ \AA}^{-1}$ focuses on the longitudinal zone-boundary phonon (see again Fig. 2 and Ref. 12), which is found at about 1.02

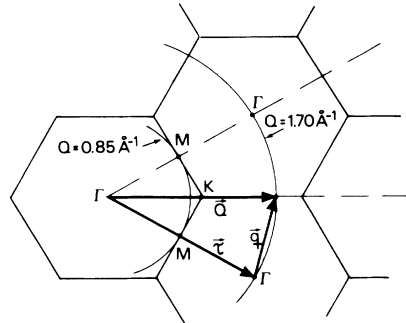


FIG. 2. The region of reciprocal space covered by the scans shown in Fig. 1. One example of a scattering triangle is sketched. It represents a case of excitation of a transverse zone-boundary phonon. Q is the total momentum transfer, τ is a reciprocal-lattice vector, and q is the phonon momentum.

THz in Fig. 1(b).

To interpret the data we evaluated a simple model considering the D_2 molecule at 4 K as a free rotor.³ Nearest-neighbor molecules of D_2 were connected by springs (spring force constant α) on a triangular grid,¹³ and each molecule was also attached at its commensurate position to the substrate by another spring (spring force constant β). These two springs are both in-plane springs. No coupling between this structure and the phonons of the substrate was taken into account as was done for the heavy rare gases.¹⁴ One has only two free parameters which are the two force constants. In a first step the coupling to the substrate *alone* can be estimated to a first approximation by our taking only the in-plane curvature of the D_2 -graphite potential at the adsorption

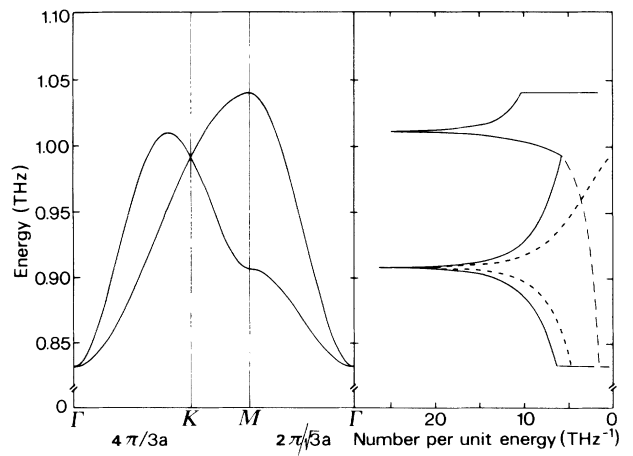


FIG. 3. (Left) Dispersion relation for the commensurate triangular lattice of D_2 on graphite and (right) the corresponding density of states. The different branches are the longitudinal (dash-dotted line) and transverse (dashed line) in-plane modes. The out-of-plane mode (not shown) lies much higher in energy and is an Einstein mode in our model (notice the expanded scale).

site. This potential has been calculated classically according to Steele¹⁵ and the resulting spring constant is $\beta=0.141 \text{ N/m}$ giving an energy for the in-plane oscillation (Einstein mode) of $\hbar\omega=0.73 \text{ THz}$, close to the value of 0.96 THz of a calculation⁶ which includes the

$$\omega^2 = (a/M_D)[3 - a - b - c \pm (a + b^2 + c^2 - ab - ac - bc)^{1/2}] + \beta/M_D, \quad (1)$$

where M_D is the mass of the D_2 molecule, $a = \cos[a_0 q_x]$, $b = \cos[(a_0/2)(\sqrt{3}q_y + q_x)]$, $c = \cos[(a_0/2)(\sqrt{3}q_y - q_x)]$, a_0 is the nearest-neighbor distance, and q_x , q_y are the components of momentum of the phonons (the q_x direction corresponds to the ΓK line; see Fig. 2).

We calculated the line shape of the spectrum at certain momentum transfers Q for the irreducible $\frac{1}{12}$ of the Brillouin zone with the dispersion relation given by formula (1) taking into account the 2D averaging, the mosaic spread of the sample around the c axis, and the resolution ellipsoid of the spectrometer. The one-phonon dynamic structure factors for the coherent and incoherent scattering were taken from Lovesey.¹⁶ D_2 has an incoherent cross section which contributes to the spectrum essentially as an additional term proportional to the density of states [see Fig. 3 and the contributions in Figs. 1(a) and 1(b)].

The mean square displacement of the D_2 molecules in the commensurate phase (used in the one-phonon dynamic structure factor) which determines the Debye-Waller factor was found in diffraction measurements¹⁷ to be $\langle u^2 \rangle_{2D} = 0.25 \text{ \AA}^2$. With use of the relation for the Debye-Waller exponent for a 2D solid in the harmonic approximation,

$$2W = Q^2 \langle u^2 \rangle_{2D} / 2 \\ = (\hbar Q^2 / 2M_D) \int d\omega Z(\omega) [2n(\omega) + 1] / \omega, \quad (2)$$

where $Z(\omega)$ is the in-plane density of states calculated from our results (Fig. 3) and $n(\omega)$ the Bose population factor, one obtains $\langle u^2 \rangle_{2D} = 0.21 \text{ \AA}^2$, in good agreement also with theoretical calculations.⁶ $Z(\omega)$ is taken in anticipation of the results given later on. A value of 0.26 \AA^2 is given in Ref. 6 (following the Hartree theory) which is very close to the previously mentioned ones. If the out-of-plane contribution of 0.04 \AA^2 (Ref. 7) is added, a value of about 0.27 \AA^2 results which can be compared with the 3D one of 0.25 \AA^2 .⁵ However, the distribution of the root mean square deviations of D_2 is anisotropic on graphite.

The 2D averaging is necessary because Papyex is not a single crystal but a 2D powder as mentioned before. The mosaicity is given by the orientational distribution of the c axis which has been described by a function of the form¹²

$$H(\theta) = H_0 + H_1 \exp[-\frac{1}{2}(\theta/\theta_m)^2], \quad (3)$$

θ being the angle between a particular adsorbing surface

quantum aspect of the system. Both values also agree roughly with the experimental data which show a peak near 0.9 THz [Fig. 1(a)]. However, much more information is gained if the adsorbate-adsorbate interaction is included. In Fig. 3 we show the calculated dispersion curve *including* this interaction:

and the scattering plane and θ_m an effective mosaic parameter. H_0 takes into account the isotropic powder part of the sample. We took $\theta_m = 30^\circ$ and $H_0 = H_1 = 0.5$ as determined from elastic diffraction measurements.¹² The principal axes of the resolution ellipsoid were calculated by an appropriate program for the curved analyzer configuration.¹⁰ The curves obtained after the averaging and folding procedure for $Q = 1.70 \text{ \AA}^{-1}$ and $Q = 0.85 \text{ \AA}^{-1}$ ($Q = k_f - k_i$) are shown together with the experimental points in Figs. 1(a) and 1(b). The fit of the curves (running the complete folding procedure as described) has been done in the following way: The two spring constants in formula (1) have been varied until a best fit was obtained for the leading edge of the excitation at the phonon gap [at $\sim 0.85 \text{ THz}$ in Fig. 1(a)] and for the longitudinal zone-boundary phonon [main peak at 1.1 THz in Fig. 1(b)]. The resulting values of the two spring constants are $\alpha = 0.016 \text{ N/m}$ and $\beta = 0.182 \text{ N/m}$. The dispersion curves and the density of states according to the two spring constants are shown in Fig. 3. In the calculation one can separate the relative contributions of the two phonon branches (Fig. 3). In this manner it is possible to assign each of the measured peaks to the contribution of the different regions of the Brillouin zone [see differently marked lines in Figs. 1(a) and 1(b)].

The calculated line shape for the spectra *before* convolution with the energy resolution of the spectrometer but including the convolution with the resolution in Q space is depicted in Fig. 1(c) for the two Q values at which the scans were performed [Figs. 1(a) and 1(b)]. In the comparison of the intensities of the two spectra in Fig. 1(c) it should be noted that the Debye-Waller factor is included in the one-phonon dynamic structure factor¹⁶ as well as the Q dependence and the molecular form factor.⁵ The signal at $Q = 0.85 \text{ \AA}^{-1}$ (longitudinal phonons), which is a double peak in Fig. 1(c), gives a single peak in Fig. 1(b) after the convolution with the instrumental resolution. The signal at $Q = 1.70 \text{ \AA}^{-1}$ in Fig. 1(c) exhibits a sharp peak at the phonon gap. The transverse phonons produce a sharp peak (0.905 THz) and a cutoff at slightly higher energies. [These two features do not coincide because the scan does not exactly cross the M point (see Fig. 2)]. The convolution with the instrumental resolution results in a broad peak in Fig. 1(a) and not in the double peak shown by the experimental data. This is because the frequency of 0.905 THz obtained in our model for the transverse zone-boundary phonon is too low com-

pared with 0.925 THz deduced from the experimental points in Fig. 1(a). To include noncentral forces or the influence of next-nearest neighbors could correct this disagreement but would on the other hand increase the number of adjustable parameters. It was our choice to keep the parameters at a minimum with a model that describes well in a qualitative way all the measured features even if there remain some quantitative differences. A more sophisticated model calculated from first principles⁷ shows the same qualitative features but presents some quantitative differences with respect to our data. In this calculation the zone-center phonon gap is found to be 0.77 THz. This has to be compared with our experimentally obtained value of 0.83 THz (with an estimated uncertainty of 0.03 THz) which indicates a stronger curvature of the in-plane D₂-graphite potential. For comparison, other values for the phonon gap are 0.96 THz (Ref. 6) and 0.73 THz from the calculation of Ref. 15. The experimental width of the density of states is 0.18 THz compared with a calculated one of 0.31 THz (Ref. 7) showing a smaller intermolecular interaction.

The present data show unambiguously that dispersion is present for the phonons of D₂ in the commensurate phase on graphite and that one can determine the two coupling constants because of the successful separation of the signal at the phonon gap and the transverse zone-boundary phonon from that of the longitudinal zone-boundary phonon by the correct choice of the two momentum transfers. The analysis yields that the coupling to neighboring molecules is nearly 10 times smaller than the in-plane coupling to the substrate due to the corrugation. This fact led in previous measurement to the assumption that the observed mode was Q independent. There is still excess intensity left which could be due to a coupling between in-plane and out-of-plane motions which has been ignored in our model, to the coupling to the substrate phonons, or to an oversimplification in the mosaic distribution of the graphite substrate [Eq. (3)].

We thank J. Eckert for helpful comments. This work has been partially supported by the West German

Federal Ministry of Research and Technique (Bundesminister für Forschung und Technologie).

¹M. Nielsen, J. P. McTague, and W. Ellenson, *J. Phys. (Paris), Colloq.* **38**, C4-10 (1977); M. Nielsen, J. P. McTague, and L. Passell, in *Phase Transitions in Surface Films*, edited by J. G. Dash and J. Ruvalds (Plenum, New York, 1980), p. 127; H. J. Lauter, H. P. Schildberg, H. Godfrin, H. Wiechert, and R. Haensel, *Can. J. Phys.* (to be published); H. P. Schildberg, H. J. Lauter, H. Freimuth, H. Wiechert, and R. Haensel, *Jpn. J. Appl. Phys. Suppl.* **26**, 345 (1987).

^{2a}H. Freimuth and H. Wiechert, *Surf. Sci.* **178**, 716 (1986).

^{2b}F. C. Motteler and J. G. Dash, *Phys. Rev. B* **31**, 346 (1985).

³P. R. Kubik, W. N. Hardy, and H. Glattli, *Can. J. Phys.* **63**, 605 (1985).

⁴J. L. Seguin and J. Suzanne, *Surf. Sci.* **118**, L241 (1982); J. Cui and S. C. Fain, Jr., *J. Vac. Sci. Technol. A* **5**, 710 (1987).

⁵M. Nielsen and H. Bjerrum Møller, *Phys. Rev. B* **3**, 4383 (1971); M. Nielsen, *Phys. Rev. B* **7**, 1626 (1973).

⁶X.-Z. Ni and L. W. Bruch, *Phys. Rev. B* **33**, 4584 (1986).

⁷A. D. Novaco, *Phys. Rev. Lett.* **60**, 2058 (1988).

⁸V. L. P. Frank, H. J. Lauter, and P. Leiderer, *Jpn. J. Appl. Phys. Suppl.* **26**, 347 (1987).

⁹Neutron beam facilities at the HFR(ILL), available for users.

¹⁰H. Kraxenberger, thesis, Universität München 1980 (unpublished).

¹¹Papex is produced by Carbon Lorraine, 45 Rue des Acacias, 75821 Paris Cedex 17, France.

¹²H. Taub, K. Carneiro, J. K. Kjems, and L. Passell, *Phys. Rev. B* **16**, 4551 (1977).

¹³U. Brandt and R. Schmidt, *Z. Phys. B* **67**, 215 (1987).

¹⁴F. W. de Wette, B. Firey, and E. de Rouffignac, *Phys. Rev. B* **28**, 4744 (1983).

¹⁵W. A. Steele, *Surf. Sci.* **36**, 317 (1973).

¹⁶S. V. Lovesey, *Theory of Neutron Scattering from Condensed Matter* (Clarendon, Oxford, 1984), Chap. 4, Eqs. 4.75 and 4.80.

¹⁷H. P. Schildberg and H. J. Lauter, private communication.